



Research Article

<https://doi.org/10.1631/jzus.B2500442>

CircMED17 regulates bovine adipogenesis and fat deposition via mediating the proliferation and differentiation of bovine adipocytes

Yuta YANG^{1*}, Shaoli ZHANG^{1*}, Lei CHEN¹, Yunan HE¹, Enhui JIANG¹, Chuanying PAN¹, Yang LI¹, Chuzhao LEI¹, Jiyao WU^{2✉}, Xianyong LAN^{1✉}

¹College of Animal Science and Technology, Northwest A&F University, Yangling, Shaanxi 712100, China

²College of Animal Science, Fujian Agriculture and Forestry University, Fuzhou 350002, China

Abstract: Fat deposition is a key factor influencing beef quality. Therefore, understanding the regulatory mechanisms of adipogenesis is crucial for improving meat production traits in cattle. Circular RNAs (circRNAs) have emerged as important post-transcriptional regulators in various biological processes, including adipocyte differentiation. In our study, circMED17 was identified as a stable, nuclear-localized circRNA derived from exons 2 and 3 of the *MED17* gene, with its expression markedly upregulated during bovine preadipocyte differentiation, suggesting its potential role in adipogenesis. Functional analyses revealed that circMED17 inhibits preadipocyte proliferation and apoptosis while promoting differentiation and lipid accumulation. Mechanistically, circMED17 exerts dual regulatory effects by sponging miR-146b as a competing endogenous RNA (ceRNA) and by directly interacting with the transcription factor GATA2. Importantly, the *in vivo* overexpression of circMED17 in obese mice increased subcutaneous fat deposition, confirming its pro-adipogenic role. Collectively, the findings reveal a previously unreported dual mechanism of circMED17 in bovine adipogenesis and highlight its potential as a molecular target for improving beef quality through genetic and breeding strategies.

Key words: Circular RNAs (circRNA); Cattle; Adipogenesis; Beef quality; Post-transcriptional regulation

1 Introduction

Fat deposition is a key factor influencing beef quality traits such as marbling, tenderness and flavor, three characteristics critical to consumer preferences and market value (Kuraz et al., 2024). However, current beef cattle breeds often struggle to meet the increasing demand for high-quality meat, highlighting the need for improved genetic strategies. Adipose tissue, mainly composed of preadipocytes and mature adipocytes, plays a central role in fat accumulation (Ferhat et al., 2019; Li et al., 2025). The proliferation, differentiation and apoptosis of preadipocytes are essential physiological processes that determine fat deposition capacity. Therefore, understanding the molecular mechanisms regulating adipose tissue development is crucial for enhancing beef quality and guiding genetic improvement strategies.

In recent years, non-coding RNAs (ncRNAs) have been recognized as important mediators of various

✉ jiyao WU, wujiyao@fafu.edu.cn

✉ Xianyong LAN, lanxianyong79@126.com

* The two authors contributed equally to this work

Jiyao WU, <https://orcid.org/0000-0002-8103-854X>

Xianyong LAN, <https://orcid.org/0000-0003-2254-5805>

Received July 29, 2025; Revision accepted Oct. 10, 2025;

Crosschecked xxx. xx, 20xx; Published online xxx. xx, 20xx

biological processes, with their roles in adipogenesis attracting particular attention (Engin et al., 2017; Ru et al., 2023; Jiang et al., 2025). Circular RNAs (circRNAs) are a recently discovered class of endogenous ncRNAs characterized by covalently closed loop structures, which confer high stability by rendering them resistant to exonuclease degradation (Zhao et al., 2022). An increasing number of studies have demonstrated that circRNAs participate in the proliferation and differentiation of adipocyte precursor cells and lipid accumulation in these cells by acting as miRNA sponges, interacting with RNA-binding proteins, or regulating the transcription of target genes (Liu et al., 2022a; Feng et al., 2022; Yang et al., 2022). Kyoto Encyclopedia of Genes and Genomes (KEGG) pathway analysis revealed a substantial number of circRNAs differentially expressed between human visceral preadipocytes and mature adipocytes, implicating their involvement in critical pathways including fatty acid synthesis and degradation (Ghafouri and Taheri, 2021; Huang and Choo, 2023). CircRNAs identified in the subcutaneous adipose tissues of Large White and Laiwu pigs were predominantly enriched in biological processes such as triglyceride (TG) catabolism, fat storage, and phosphatidic acid biosynthesis (Yousuf et al., 2022). In fact, numerous studies have confirmed that circRNAs play crucial roles in regulating the adipogenic differentiation of preadipocytes. For example, CircFUT10 promotes the proliferation of bovine preadipocytes while inhibiting their differentiation by upregulating *PPAR γ* and subsequently activating *PPARGC1B* (Jiang et al., 2020). Furthermore, the expression of circBDP1 is initially very low during early bovine adipocyte differentiation but gradually increases as differentiation progresses. The overexpression of circBDP1 in bovine adipocytes enhances the expression of proliferation marker genes, consistent with observed increases in cell proliferation, and also promotes adipocyte differentiation (Zhang et al., 2022). CircBTBD7, predominantly localized in the cytoplasm of bovine preadipocytes, inhibits adipogenesis by sponging miR-183 and thereby modulating the expression of the *SMAD4* gene, functioning through the miR-183/*SMAD4* regulatory axis (Ma et al., 2023). Moreover, circFLT1 and circINSR have both been shown to influence bovine adipocyte proliferation, differentiation and apoptosis, albeit with distinct regulatory effects. Functional analyses have revealed that circFLT1 overexpression simultaneously promotes adipocyte proliferation and differentiation while reducing apoptosis. Conversely, circINSR overexpression enhances proliferation and inhibits apoptosis but exerts an inhibitory effect on adipogenic differentiation, as evidenced by Oil Red O and BODIPY staining (Kang et al., 2020; Zhao et al., 2023). These findings provide new insights into the molecular mechanisms underlying adipogenesis, that is, circRNAs finely regulate the biological processes of preadipocytes through multiple mechanisms, playing a critical role in adipose development and metabolic regulation.

Although numerous studies have revealed the regulatory roles of circRNAs in adipogenesis, functional investigations of circRNAs in bovine adipose tissue remain limited, particularly regarding the systematic validation and mechanistic dissection of key circRNA molecules. Given that beef quality is highly dependent on fat deposition, elucidating the regulatory network of circRNAs in the proliferation and differentiation of bovine preadipocytes and lipid accumulation therein is of great significance for uncovering the molecular mechanisms underlying adipose development, as well as for advancing genetic selection and meat quality improvement in beef cattle. Therefore, the present study aimed to identify and functionally characterize key circRNAs involved in bovine adipocyte development. Using both *in vivo* and *in vitro* approaches, we systematically evaluated the regulatory roles of circRNAs in preadipocyte biology and explored their underlying molecular mechanisms, with the ultimate goal of providing novel molecular targets and theoretical foundations for improving beef quality. Based on our previous high-throughput circRNA sequencing of bovine preadipocytes at differentiation days 0, 6 and 13 (Zhang et al., 2022), we identified circMED17 (circBase ID: bta_circ_00013260) as a highly expressed candidate in bovine adipose tissue. CircMED17 is derived from exons 2 and 3 of the *MED17* gene. Through a series of functional assays, we demonstrated that circMED17 plays a significant role in regulating the proliferation, differentiation and apoptosis of bovine preadipocytes, thereby affecting adipose tissue development and lipid accumulation. These findings suggest that circMED17 may serve as an important molecular regulator of bovine adipogenesis and contribute to a deeper understanding of the molecular mechanisms governing the formation of quality beef.

2 Materials and methods

2.1 Sample collection and screening of circMED17

In order to isolate and culture preadipocytes and perform tissue analysis, adipose tissue, along with the heart, liver, lung, kidney, small intestine, and muscle, was collected from 3-month-old fetal Qinchuan cattle ($n=3$) from the Yangling Branch of Shaanxi Qinbao, Shaanxi Province, China. The samples were collected under strict aseptic conditions, immediately snap-frozen in liquid nitrogen and stored at -80°C . The RNA sequencing data for circRNA screening were further integrated, analyzed and mined based on the circRNA sequencing results of our laboratory. CircMED17 was highly expressed during the late stage of adipogenic differentiation, with a significantly higher expression level in mature adipocytes compared to preadipocytes; therefore, it was selected as a key candidate molecule for further investigation in this study.

2.2 Isolation, culture of bovine preadipocytes, and adipogenic differentiation

The isolation of bovine preadipocytes was performed as previously described (Wu et al., 2022). Briefly, subcutaneous adipose tissue was collected from 3-month-old fetal Qinchuan cattle. Tissue blocks were washed twice with 75% ethanol, followed by PBS containing 200 U/mL penicillin and 200 $\mu\text{g}/\text{mL}$ streptomycin. After cleaning, the blocks were finely minced with ophthalmic scissors in a culture dish, and a small volume of preadipocyte culture medium (DMEM/F-12 high-glucose supplemented with 20% fetal bovine serum, 100 U/mL penicillin and 100 $\mu\text{g}/\text{mL}$ streptomycin) was optionally added. For enzymatic digestion, a collagenase type I solution (2 mg/mL; equivalent to 100 mg dissolved in 50 mL of DMEM/F-12 high-glucose medium) was prepared. The digestion mixture (10 mL) was transferred to a sealed centrifuge tube and incubated in a shaking incubator at 37°C and 180 r/min for approximately 2.5 h. Following digestion, samples were centrifuged at 800 r/min for 5 min at room temperature, and the resulting cell pellet was collected. Isolated cells were cultured at 37°C in a humidified atmosphere with 5% CO_2 . After 24 h, evenly distributed bovine preadipocytes were observed under a microscope. Subculturing was initiated when cells reached approximately 80% confluence. To induce adipogenic differentiation, preadipocytes were cultured to full confluence and then incubated in differentiation medium consisting of DMEM/F-12 high-glucose supplemented with 10% fetal bovine serum, 100 U/mL penicillin and 100 $\mu\text{g}/\text{mL}$ streptomycin, 5 $\mu\text{g}/\text{mL}$ insulin, 1 $\mu\text{mol}/\text{L}$ dexamethasone, 0.5 mmol/L 3-isobutyl-1-methylxanthine (IBMX), and 1 μM rosiglitazone for the first two days. Thereafter, cells were maintained in a medium containing 5 $\mu\text{g}/\text{mL}$ insulin, which was refreshed every two days until large lipid droplets were observed.

2.3 RNase R digestion identification and actinomycin D detection of RNA stability

In order to validate the circular structure of the candidate circRNA, total RNA extracted from bovine preadipocytes was treated with RNase R (20 U/ μL) at 3–4 U per μg RNA. Untreated total RNA served as the control. After incubation at 37°C for 15 min, reverse transcription was performed on both treated and untreated RNA samples. Subsequently, quantitative reverse transcription PCR (qRT-PCR) was carried out to assess the expression levels of the circRNA, its corresponding linear messenger RNA (mRNA), and the housekeeping gene Glyceraldehyde-3-phosphate dehydrogenase (*GAPDH*). For RNA stability analysis, actinomycin D (dissolved in dimethyl sulfoxide (DMSO)) was added to bovine preadipocytes at ~80% confluence to achieve a final concentration of 2 mg/mL. Cells were harvested at 0, 4, 8, 12, and 24 h post-treatment. Total RNA was extracted at each time point, and qRT-PCR was used to measure the expression levels of the circRNA and its linear host transcript to evaluate RNA stability dynamics. All qRT-PCR reactions were performed using gene-specific primers, with their sequences listed in Table 1.

Table 1 Primers of RT-qPCR

Name	Primer pairs sequences(5'-3')	Amplification length (bp)
<i>MED17</i> mRNA	F:GAGTAGGACTGCTGCAACCA R:GACCCGGATCTGCTCAACTC	190
circMED17	F:TGAGATTGAGGCAACACTGGA R:TCTCTGTCAGGGCACTTCTC	150
pre-bta-miR-93	F:CGCGGATCCGCTTCATTTCTGTCCTCACGC R:CCCAAGCTTCACCACGAGATGGAGCTTGG	173
pre-bta-miR-146a	F:CGCGGATCCGATGAGGGTCTTTGTGCCA R:CCCAAGCTTTTCCAAGTTCTCCAGCCGAC	185
pre-bta-miR-146b	F:CGCGGATCCCTGGGGATGAGGAAAGATTCA R:CCCAAGCTTCAACTGGCTGATGCCCCGT	200
<i>GAPDH</i>	F:TGAGGACCAGGTTGTCTCTCTGCG	145

	R:CACCACCCTGTTGCTGTAGCCA	
	F:GCTTCGGCAGCACATATACTAAAAT	
<i>U6</i>	R:CGCTTCACGAATTTGCGTGTTCAT	89

2.4 Total RNA extraction, cDNA synthesis and qRT-PCR

Total RNA was extracted from the collected tissues using the standard chloroform-isopropanol method (Toni et al., 2018). The quality and concentration of the RNA were assessed, and high-quality RNA was reverse-transcribed into cDNA. QRT-PCR was performed to profile circRNA expression using *GAPDH* as an internal reference. Primers were designed with NCBI Primer-BLAST, with their sequences listed in Table 2. Relative gene expression was calculated using the $2^{-\Delta\Delta Ct}$ method.

Table 2 qPCR Primers of target genes

Name	Primer pairs sequences(5'-3')	Amplification length (bp)
<i>Cyclin D1</i>	F:CCGTCCATGCGGAAGATC R:CAGGAAGCGGTCCAGGTAG	108
<i>Cyclin E1</i>	F:CTTCGGGCTTGAGGTCTGAT R:ATGGTATCCGGTTCCTTCGC	79
<i>Cyclin B1</i>	F:GGTGAATGGACACCAACTCT R:CCACGGTTCACCATGACCA	104
<i>CDK2</i>	F:TTTGCTGAGATGGTGACCCG R:TAACCTCTGGCCAAACCACC	115
<i>Bax</i>	F:GAGATGAATTGGACAGTAACA R:TTGAAGTTGCCGTCAGAA	118
<i>Bcl2</i>	F:ATGACCGAGTACCTGAAC R:CATACAGCTCCACAAAGG	79
<i>Bclxl</i>	F:ACCCAGGGACAGCATATCA R:CCAAGTTGCGATCCGACTCA	165
<i>Caspase 3</i>	F:TCAGTCAGTCAGTTGGGCAC R:ACACACCCGTAGCTGTGAAG	149
<i>Caspase 8</i>	F:AGGTCTTTTCCCAAGCTATCC R:AAGCTGAAAAGGGAGTTTGGGA	144
<i>p21</i>	F:AGGGCACGTCTCAGGAGGA R:CAGTCTGCGTTTGGAGTGGTAG	164
<i>p53</i>	F:ACTTGTGGAACCTACTTCCTGA R:GGCAACATCTGTGTACGGGA	89
<i>CEBPa</i>	F:TTCAACGACGAGTTCCTGGC R:TAGTCAAAGTCGTTGCCGCC	101
<i>CEBPβ</i>	F:GACAAGCACAGCGACGAGTA R:GCGTCTTGAACAAGTTCCGC	199
<i>FABP4</i>	F:TGTCACCTGCCACCAGAGTTT R:TGGACAACGTATCCAGCAGA	102
<i>PPARγ</i>	F:ACTCATTGGTGCGTTCCCAA R:AACAGGGATTTGCCACGACT	112

2.5 Vector construction, synthesis of interfering fragments and cell transfection

The target fragment and the pcDNA2.1 vector were double-digested with the restriction endonucleases *KpnI* and *BamHI* (Takara, Dalian). The linearized vector and the target fragment were ligated using T4 DNA ligase to construct the recombinant plasmid, which was subsequently transformed into competent *Escherichia coli* (*DH5α*) and cultured in LB medium. Single colonies were selected for bacterial PCR, followed by agarose gel electrophoresis and Sanger sequencing to verify successful construction. The confirmed circMED17 overexpression vector was preserved for laboratory use. Additionally, small interfering RNAs (siRNAs) specifically targeting the reverse splicing sites of circMED17 were synthesized by GenePharma (Shanghai, China) to inhibit its function.

2.6 Western blotting

Cells were lysed by adding high-efficiency RIPA lysis buffer (Beyotime) supplemented with 1 mM

PMSF, followed by incubation at 4°C for 20–30 min to ensure complete lysis. Cells were then gently scraped and collected into 1.5 mL centrifuge tubes. The lysates were centrifuged at low temperature to remove cellular debris, and the resulting supernatants containing total protein were collected. The protein concentrations were determined using a BCA assay, then equal amounts of protein were mixed with 5× SDS-PAGE loading buffer and denatured by boiling. Samples were stored at -80°C until further use. For Western blotting, proteins were separated on polyacrylamide gels by SDS-PAGE at 120 V for 2 h and then transferred onto PVDF membranes at 200 mA for 2 h. Membranes were blocked for 2 h with 0.05 g/mL non-fat milk or a commercial blocking solution and incubated overnight at 4°C with primary antibodies. After three washes with TBST, the membranes were incubated with appropriate secondary antibodies at room temperature for 2 h, followed by three additional washes. Protein bands were visualized using a chemiluminescent imaging system.

2.7 cell counting kit-8 (CCK-8) assay and 5-ethynyl-2'-deoxyuridine (EdU) assay for the detection of adipocyte proliferation

Bovine preadipocyte proliferation was assessed using CCK-8 and EdU assays. For the CCK-8 assay, cells were seeded in 96-well plates at a density of 5×10^3 cells per well, with 10 replicates per treatment group, and incubated at 37°C with 5% CO₂ for 24 h. Next, 10 µL of CCK-8 solution (Dojindo, Japan) was added to each well, and the plates were incubated for an additional 1.5–2.5 h. Absorbance at 450 nm was immediately measured using a microplate reader, and cell viability was calculated relative to the negative control after subtracting the blank values. For the EdU assay, cells were seeded in 96-well plates with four replicates per group. After 24 h of plasmid transfection, EdU solution (Guangzhou RiboBio Co., Ltd.) was diluted 1:100 in culture medium, and 100 µL was added to each well for a 2-hour incubation period. Cells were fixed with 50 µL of 0.04 g/mL paraformaldehyde for 30 min at room temperature, followed by quenching with 50 µL of 2 mg/mL glycine. Subsequently, cells were permeabilized with 100 µL of PBS containing 0.5% Triton X-100 for 10 min on a gentle shaker. Apollo staining was performed according to the manufacturer's instructions and cell proliferation was assessed under an inverted fluorescence microscope.

2.8 Flow cytometry was used to detect the proliferation and apoptosis of adipocytes

In order to assess proliferation and apoptosis via flow cytometry, bovine preadipocytes were cultured in 60 mm dishes. For cell cycle analysis 24 h post-transfection, cells were detached using trypsin, washed three times with pre-cooled PBS and resuspended. Cells were then fixed in 70% ethanol at -20°C. After staining with a cell cycle detection kit, cell cycle distribution was analyzed by flow cytometry to evaluate proliferation. For apoptosis analysis, cells were similarly harvested 24 h post-transfection using trypsin (without EDTA), washed three times with PBS at 37°C, and resuspended. Apoptotic cells were detected using an Annexin V-APC/7-AAD kit according to the manufacturer's instructions.

2.9 Oil Red O staining for detection of adipocyte differentiation

In order to assess adipogenic differentiation, bovine preadipocytes were cultured in 24-well plates with three replicates per treatment group for Oil Red O staining. Lipogenic differentiation was induced 4–6 h after transfection when the cell confluence exceeded 90%. After 6 days of differentiation, cells were stained following the manufacturer's protocol (Beijing Solarbio Science & Technology Co., Ltd.). Stained cells were examined under an inverted microscope. Nuclei were counterstained with DAPI and observed under a fluorescence channel, while lipid droplets in mature adipocytes were visualized as red under bright-field illumination. The extent of adipogenic differentiation was evaluated based on the presence and accumulation of lipid droplets.

2.10 Terminal deoxynucleotidyl transferase dUTP Nick-End Labelin (TUNEL) assay for the detection of adipocyte apoptosis

Apoptosis was assessed using the TUNEL assay. Bovine preadipocytes were cultured in 96-well plates, with four replicates per group. Staining was performed according to the manufacturer's instructions (Guangzhou RiboBio Co., Ltd.). Cells were examined under an inverted fluorescence microscope: nuclei were counterstained with Hoechst 33342 (blue fluorescence), and apoptotic cells exhibited red fluorescence indicative of DNA fragmentation. Apoptosis was quantified as the percentage of TUNEL-positive cells relative to the total cell number.

2.11 Dual-luciferase reporter assay

The luciferase reporter assay was employed to validate specific nucleic acid interactions. HEK293T cells were seeded in 96-well plates, with six replicates per treatment group. CircRNA fragments containing putative miRNA binding sites and their corresponding mutant constructs were cloned into the psi-CHECK2 vector.

Plasmids and miRNA mimics were co-transfected into the cells according to the experimental design. Twenty-four hours post-transfection, cells were harvested for the dual-luciferase assay to measure firefly luciferase activity using firefly luciferin and Renilla luciferase activity using the specific substrate provided in the Dual-Luciferase® Reporter Assay System (Promega) while following the manufacturer's instructions.

2.12 RNA Immunoprecipitation (RIP) Assay

RNA immunoprecipitation (RIP) was performed to investigate protein-RNA interactions. This method uses antibodies specific to a target protein to pull down the RNA-binding protein (RBP) along with the RNAs directly associated with it, enabling the subsequent verification and analysis of these interactions. In this study, bovine preadipocytes were cultured in 150 mm dishes and subjected to appropriate transfection. Cells were then washed, trypsinized and lysed to obtain cell lysates for RIP. Next, the binding of CircMED17 to predicted microRNAs (miRNAs) and proteins was assessed. All downstream steps, including antibody validation, magnetic bead incubation, RNA purification, qRT-PCR, and western blotting, were conducted following the Magna RIP™ RNA-Binding Protein Immunoprecipitation Kit protocol (Millipore, USA).

2.13 *In vivo* animal experiments

High-fat model mice (db/db), which have been widely used for adipose tissue research, were obtained from Cyagen Biosciences. Three experimental groups were established: a 0.9% NaCl control group, a pcDNA2.1 empty vector group, and a CircMED17 treatment group. Nine mice were included in this study, divided into three biological replicates of three mice each. Inguinal white adipose tissue was injected daily for 15 consecutive days, with the respective plasmid complexed with an *in vivo* transfection reagent, following the manufacturer's dosage guidelines. At the end of the treatment period, the inguinal white adipose tissue was harvested, fixed and embedded in paraffin. Tissue sections (5 μm) were prepared using a microtome and subjected to standard histological procedures, including dewaxing, staining, dehydration, permeabilization and mounting. Histological analysis was performed under bright-field illumination using an inverted microscope.

2.14 Statistical Analysis

Data analysis and visualization were conducted using SPSS 22 and GraphPad Prism 8. An independent-sample t-test was used to assess the significance of two-group data, while one-way ANOVA was performed to evaluate multi-group data, with * $P < 0.05$ denoting significant difference and ** $P < 0.01$ denoting extremely significant difference.

3 Results

3.1 Structural identification, tissue expression and temporal expression characteristics of bovine circMED17

Based on previous sequencing data, multiple differentially expressed candidate circRNAs were identified (Zhang et al., 2022). Among them, circMED17 was upregulated during the late stage of bovine preadipocyte differentiation, suggesting that it may act as a potential regulator of adipose tissue development. The full-length sequence and back-splice junction of circMED17 were obtained by PCR amplification. Sequence alignment revealed that circMED17 is generated by the circularization of exons 2 and 3 of the *MED17* gene. To verify its circular structure, both convergent and divergent primers were designed. Divergent primers amplified a specific product in cDNA, whereas only minimal amplification was observed in genomic DNA (gDNA), supporting the circular nature of circMED17 (Figs. 1a and 1b). Actinomycin D inhibits transcription by interfering with mRNA synthesis in cells. The results showed that with increasing treatment time, the relative mRNA expression level of the *MED17* gene significantly decreased ($P < 0.01$), whereas the expression level of circMED17 remained stable (Fig. 1c), further supporting its circular structure. RNase R is an exonuclease that digests nearly all linear RNAs, while circRNAs with a stable secondary structure are resistant to digestion. Following RNase R treatment, qRT-PCR was used to assess the expression of circMED17, *GAPDH* and *MED17*. The results indicated that *GAPDH* and *MED17* levels decreased significantly, whereas circMED17 expression remained largely unchanged (Fig.1d), further confirming that circMED17 is a circular RNA. Nucleocytoplasmic fractionation revealed that *GAPDH* was predominantly expressed in the cytoplasm, whereas U6 was mainly localized in the nucleus. The subcellular distribution of circMED17 closely resembled that of U6, indicating that circMED17 is primarily nuclear, with a fraction also present in the cytoplasm (Fig.1e). These results suggest that circMED17 may function in both the nucleus and

the cytoplasm. Total RNA was extracted from the heart, liver, lung, kidney, small intestine, adipose tissue, and muscle of Qinchuan fetal calves. qRT-PCR analysis showed that circMED17 expression was the highest in fetal adipose tissue, significantly exceeding that in the heart (Fig.1f). Temporal expression analysis indicated that circMED17 gradually increased during the proliferation of bovine adipocytes (Fig.1g) and continued to rise throughout adipocyte differentiation, reaching its peak on day 12 of differentiation (Fig.1h).

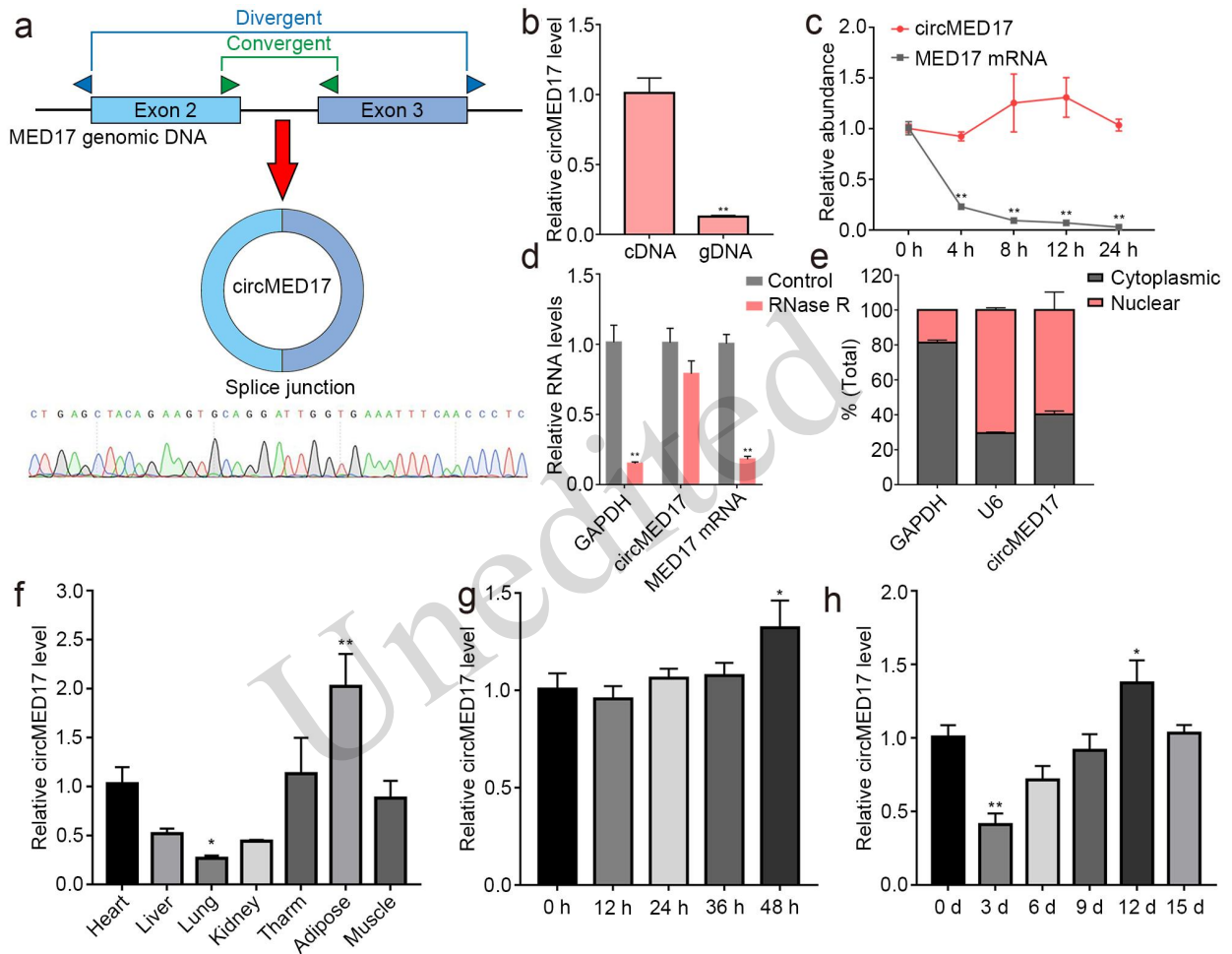


Fig. 1 Characterization and expression profiling of circMED17 in bovine adipose tissue and adipocytes.

- (a) Structural diagram of circMED17 and Sanger sequencing validation of back-splice junction.
 (b) Detection of circMED17 in cDNA and genomic DNA (gDNA) using divergent primers.
 (c) Stability of circMED17 and *MED17* in bovine primary adipocytes treated with or without 2 mg/mL actinomycin D (Act D) for 0, 4, 8, 12, and 24 hours, as determined by qPCR.
 (d) qPCR analysis of *GAPDH*, circMED17 and linear *MED17* expression in samples subjected to RNase R treatment.
 (e) Subcellular localization of circMED17 in bovine adipocytes determined by nuclear and cytoplasmic fractionation, followed by qPCR.
 (f) Expression levels of circMED17 in different bovine tissues.
 (g) qPCR analysis of circMED17 expression in bovine preadipocytes at 0, 12, 24, and 48 hours of proliferation.
 (h) qPCR analysis of circMED17 expression in bovine preadipocytes during differentiation at days 0, 3, 6, 9, 12, and 15.

3.2 Regulatory role of circMED17 in preadipocyte proliferation

In order to investigate the functional role of circMED17 in bovine adipocytes, overexpression and siRNA interference vectors were constructed. A qRT-PCR assay performed 48 hours post-transfection confirmed the successful overexpression and knockdown of circMED17 in primary bovine adipocytes (Fig. 2a). The CCK-8 assay results showed that circMED17 overexpression significantly reduced adipocyte viability, whereas its knockdown enhanced cell viability (Fig. 2b). Consistently, circMED17 overexpression suppressed the mRNA

expression of proliferation-related genes *cyclin D1* and *cyclin E1*, while silencing circMED17 led to their upregulation (Fig. 2c). Western blot analysis further confirmed these results, showing that circMED17 overexpression reduced the protein levels of cyclin D1 and cyclin E1, whereas its knockdown increased their expression (Figs. 2d and 2f). Flow cytometry analysis revealed a significant decrease in the proportion of S phase cells after circMED17 overexpression, indicating suppressed DNA synthesis and reduced adipocyte proliferation. In contrast, circMED17 knockdown increased the proportion of S phase cells, suggesting enhanced DNA synthesis and proliferative activity (Figs. 2e and 2g). EdU staining further confirmed that circMED17 overexpression significantly reduced the number of EdU-positive cells, whereas circMED17 knockdown markedly increased their number (Figs. 2h and 2i). Collectively, these results indicate that circMED17 functions as an inhibitor of bovine adipocyte proliferation: it suppresses cell cycle progression and reduces cellular proliferation capacity.

Unedited

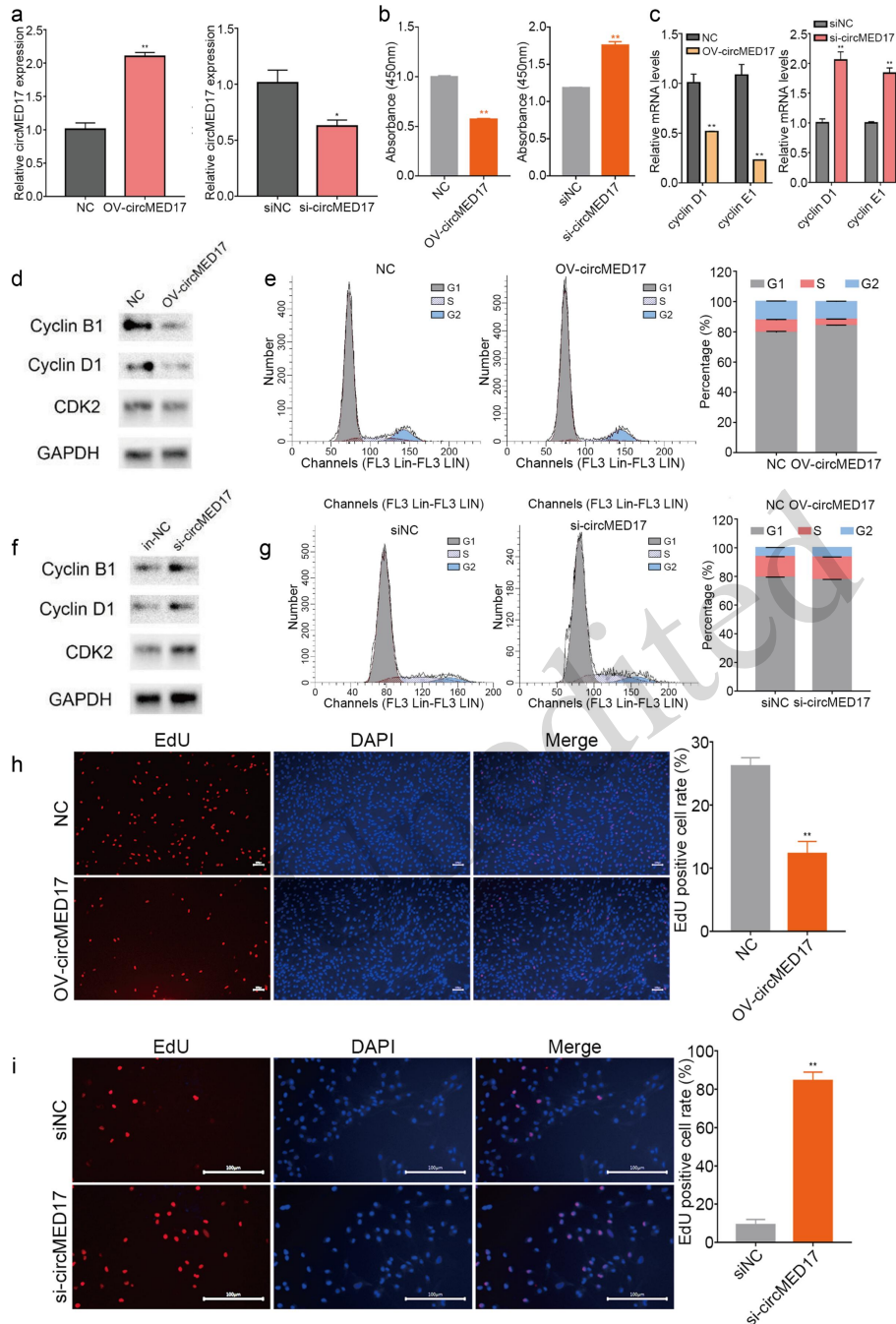


Fig. 2 CircMED17 regulates proliferation and cell cycle progression in bovine primary adipocytes.

(a) CircMED17 expression was efficiently increased by overexpression plasmid and reduced by siRNA-mediated knockdown in bovine primary adipocytes.

(b) CCK-8 assay of bovine primary adipocytes following circMED17 overexpression or si-circMED17.

(c) qPCR analysis of *cyclin D1* and *cyclin E1* expression in bovine adipocytes 48 hours after transfection with circMED17-overexpression vector and si-circMED17.

(d) Western blot analysis of CDK2, cyclin B1, and cyclin D1 protein levels in bovine adipocytes after circMED17 overexpression.

(e) Cell cycle distribution of bovine adipocytes was analyzed by flow cytometry following circMED17 overexpression (n=3).

(f) Western blot analysis of CDK2, cyclin B1, and cyclin D1 protein levels in bovine adipocytes after si-circMED17 transfection.

(g) Cell cycle distribution of bovine adipocytes was analyzed by flow cytometry following si-circMED17 (n=3).

(h, i) EdU assay of bovine adipocytes following circMED17 overexpression (h, scale bar: 10 μ m) and si-circMED17(i, scale bar: 100 μ m).

3.3 Promotion of bovine preadipocyte differentiation by circMED17

The circMED17 overexpression vector (ov-circMED17) and siRNA targeting circMED17 were transfected into bovine primary adipocytes, followed by the induction of differentiation. Real-time quantitative PCR analysis confirmed efficient overexpression and knockdown, with circMED17 expression nearly doubled in the overexpression group compared to controls and significant suppression observed in the knockdown group, meeting the requirements for subsequent experiments (Figs. 3a and 3c). The expression changes of adipocyte differentiation marker genes were assessed at both the transcriptional and the protein levels. Following circMED17 overexpression, the mRNA and protein levels of CCAAT/enhancer-binding protein α (CEBP α), CCAAT/enhancer-binding protein β (CEBP β) and peroxisome proliferator-activated receptor γ (PPAR γ) were significantly upregulated and the mRNA expression of fatty acid-binding protein 4 (*FABP4*) was also markedly increased (Figs. 3b and 3e). After circMED17 knockdown, the mRNA and protein levels of CEBP α and CEBP β were significantly reduced, the mRNA expression of (*FABP4*) was also significantly decreased, and the protein level of PPAR γ was markedly lowered (Figs. 3d and 3g). Oil Red O staining demonstrated that circMED17 overexpression enhanced lipid droplet formation and accumulation in bovine primary adipocytes, whereas si-circMED17 interference inhibited these processes (Figs. 3f and 3h). Collectively, these results indicate that circMED17 promotes the differentiation of bovine primary adipocytes.

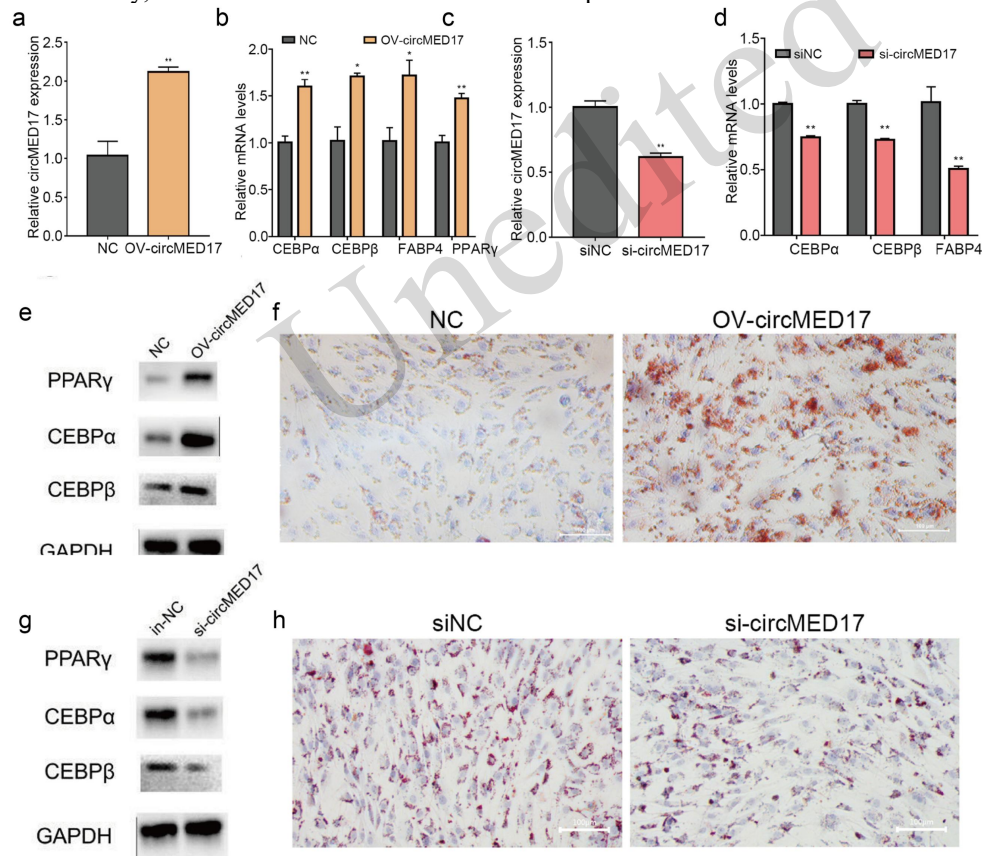


Fig. 3 CircMED17 promotes adipogenic differentiation in bovine primary adipocytes.

- (a, b) qPCR analysis confirmed the efficient overexpression of circMED17 in bovine adipocytes (a), which significantly upregulated the mRNA expression of adipogenic markers *C/EBP α* , *C/EBP β* , *FABP4*, and *PPAR γ* (b).
(c, d) qPCR confirmed the effective knockdown of circMED17 following si-circMED17 transfection (c), which led to a marked reduction in *C/EBP α* , *C/EBP β* , and *FABP4* mRNA expression in bovine adipocytes (d).
(e) Western blot analysis of adipogenic proteins showed that circMED17 overexpression increased the levels of PPAR γ , C/EBP α and C/EBP β .
(f) Oil Red O staining revealed enhanced lipid accumulation in adipocytes overexpressing circMED17 (scale bar: 100 μ m).
(g) Western blot analysis of adipogenic proteins showed that si-circMED17 reduced the levels of PPAR γ , C/EBP α , and C/EBP β .
(h) Oil Red O staining revealed reduced lipid accumulation in adipocytes with circMED17 knockdown (scale bar: 100 μ m).

3.4 Inhibition of bovine preadipocyte apoptosis by circMED17

In order to investigate the potential role of circMED17 in regulating adipocyte apoptosis, the expression levels of apoptosis-related marker genes were examined in bovine primary adipocytes following the successful overexpression or knockdown of circMED17. The qRT-PCR analysis revealed that circMED17 overexpression significantly reduced the mRNA levels of *p21*, *p53*, and *Caspase 8* compared to the control group, while the expression levels of *Bcl2* and *Bax* also showed a decreasing trend (Fig. 4a). Western blot analysis revealed that the protein expression levels of pro-apoptotic markers Bax and Bad were significantly decreased following circMED17 overexpression (Fig. 4c). Conversely, qRT-PCR analysis demonstrated that circMED17 knockdown significantly upregulated the expression of apoptosis-related genes, including *Bax*, *p21*, *p53*, *Bcl-xL*, and *Caspase 3* (Fig. 4b). Consistently, western blot analysis confirmed the increased protein levels of the pro-apoptotic markers Bax and Bad following circMED17 inhibition (Fig. 4d). These findings were further supported by TUNEL staining, which showed a significantly lower proportion of TUNEL-positive cells in the circMED17 overexpression group. Although the knockdown group exhibited an increasing trend in TUNEL-positive cells, the difference was not statistically significant (Figs. 4e and 4f). Annexin V/PI double-staining followed by flow cytometry revealed that circMED17 overexpression significantly reduced the apoptosis rate of bovine primary adipocytes, whereas circMED17 knockdown markedly increased apoptosis (Fig. 4g and 4h). Collectively, these results suggest that circMED17 inhibits apoptosis in bovine primary adipocytes.

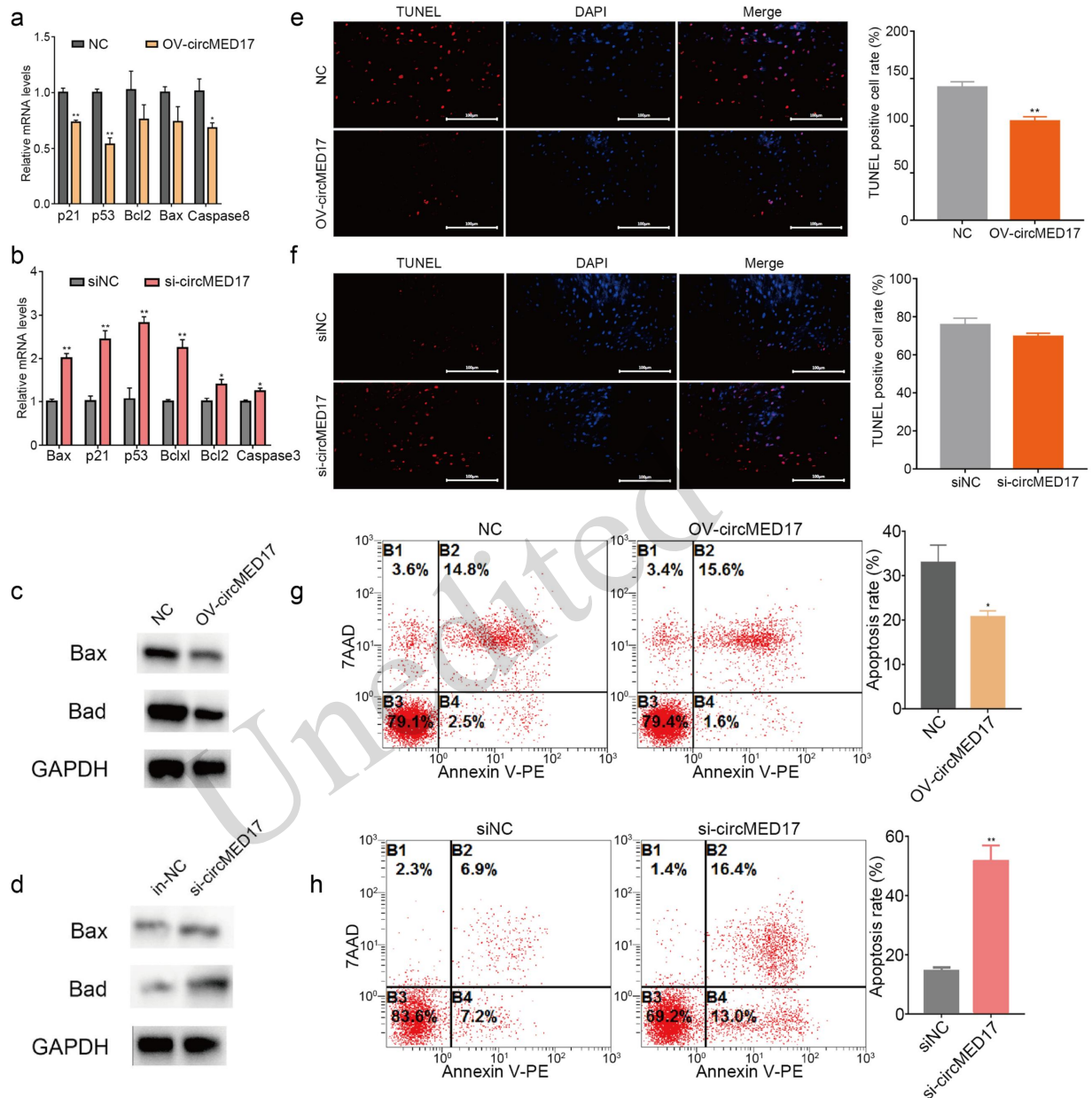


Fig. 4 circMED17 modulates apoptosis and the expression of apoptosis-related genes in bovine adipocytes.

(a) qPCR analysis of mRNA expression levels of *p21*, *p53*, *BCL2*, *BAX*, and *caspase-8* in bovine adipocytes after overexpression of circMED17.

(b) qPCR analysis of mRNA expression levels of *BAX*, *P21*, *P53*, *BCL-XL*, *BCL2*, and *caspase-3* in bovine adipocytes after transfection with si-circMED17.

(c, d) Western blot analysis of the pro-apoptotic proteins BAX and BAD in bovine adipocytes after circMED17 overexpression (c) and si-circMED17 knockdown (d).

(e, f) TUNEL staining showing apoptotic cells in bovine adipocytes after circMED17 overexpression (e) and si-circMED17 knockdown (f) (scale bar: 100 μm).

(g, h) Flow cytometry analysis of apoptosis in bovine adipocytes after circMED17 overexpression (g) and si-circMED17 knockdown (h)(n=3).

3.5 Molecular mechanism of circMED17 involving GATA2 and bta-miR-146b

Binding sites between circMED17 and candidate miRNAs were predicted using bioinformatics databases, including RNAhybrid (<https://bibiserv.cebitec.uni-bielefeld.de/rnahybrid>) (Krüger and Rehmsmeier, 2006).

Three candidate miRNAs—miR-146a, miR-93, and miR-146b—were screened and their corresponding vectors were constructed for further validation (Figs. 5a-5c). Based on the mature sequences of these miRNAs, wild-type and mutant dual-luciferase reporter vectors for circMED17 were constructed. The dual-luciferase assay showed a significant decrease in relative luciferase activity when the miR-146b overexpression vector was co-transfected with the wild-type circMED17 reporter, indicating a direct interaction between miR-146b and circMED17. In contrast, co-transfection with miR-93 or miR-146a did not result in a statistically significant reduction in luciferase activity, suggesting no direct binding between these miRNAs and circMED17 (Figs. 5d-5f). Western blot analysis of the immunoprecipitated samples confirmed the successful pull-down of AGO2 and GATA2 proteins, while no corresponding bands were detected in the IgG control group, indicating the specificity of the antibodies used for RIP (Fig. 5g). Subsequent RIP assays demonstrated that circMED17 was significantly enriched in complexes precipitated by both AGO2 and GATA2 antibodies compared to the IgG control, confirming its interaction with these proteins (Fig. 5h). Moreover, qRT-PCR analysis revealed that miR-146b levels in the AGO2 immunoprecipitate were approximately 1.6-fold higher than in the control group, supporting a direct association between miR-146b and AGO2 (Fig. 5i). These findings collectively suggest that circMED17 interacts with RNA-binding proteins AGO2 and GATA2, potentially facilitating its role in post-transcriptional regulation via miRNA-mediated mechanisms.

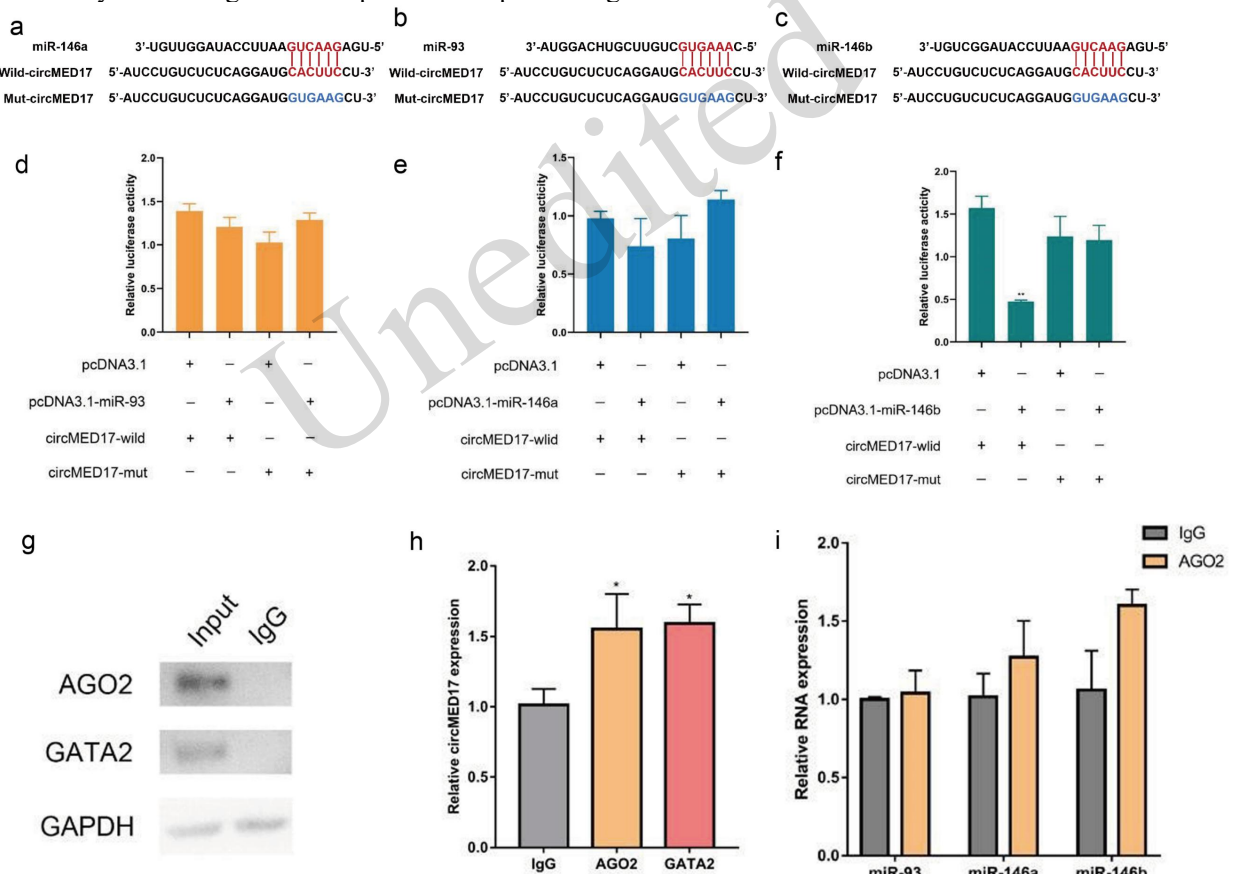


Fig. 5 CircMED17 targets GATA2 protein and binds to bta-miR-146b

(a-c) Construction of the circMED17 dual fluorescence vector according to the sequence of miR-146a (a), miR-93 (b) and miR-146b (c).

(d-f) Dual-luciferase reporter assays showing the interaction of circMED17 with miR-146a (d), miR-93 (e), and miR-146b (f).

(g) Validation of AGO2 and GATA2 antibody specificity by western blot analysis in bovine adipocytes.

(h, i) RIP assays showing the enrichment of circMED17 in AGO2 and GATA2 complexes (h), and the association of miR-146a, miR-93 and miR-146b with AGO2 (i). immunoglobulin G (IgG) was used as a negative control.

3.6 *In vivo* experiments demonstrated that circMED17 promotes adipose tissue development

The inguinal white adipose tissue of C57BL/6 mice with high-fat diet-induced obesity was locally injected with a circMED17 overexpression vector combined with an *in vivo* transfection reagent for 15

consecutive days. Subsequently, inguinal white adipose tissue samples were collected from the 0.9% NaCl control group, the pcD2.1 empty vector group, and the circMED17 overexpression group, followed by tissue fixation, paraffin embedding, and hematoxylin and eosin (H&E) staining. Histological analysis by H&E staining showed that the overexpression of circMED17 led to a significant increase in adipocyte size in the inguinal white adipose tissue of high-fat diet-induced obese mice (Figs. 6a and 6b). This study is the first to provide consistent evidence, from both *in vivo* and *in vitro* experiments, that circMED17 promotes adipocyte differentiation, thereby enhancing adipogenesis and fat deposition (Fig. 7).

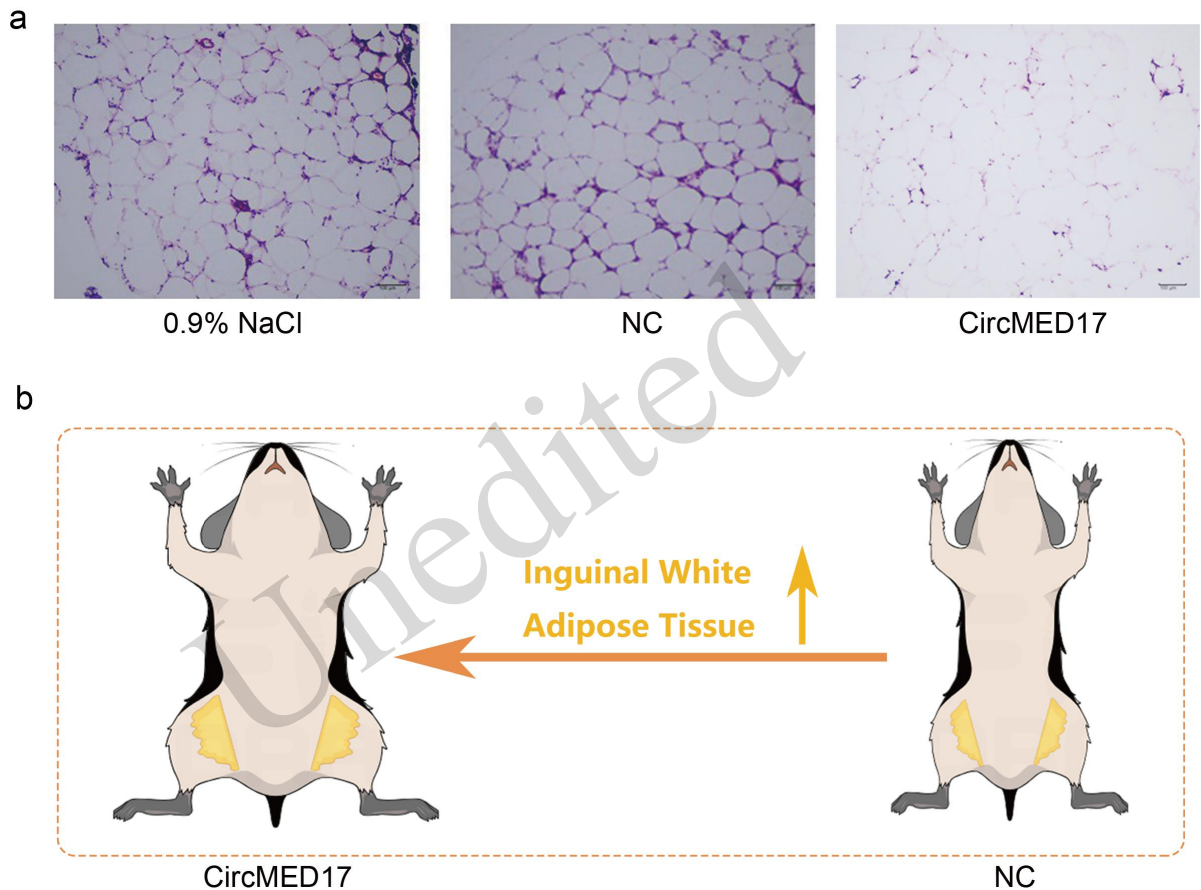


Fig.6 *In vivo* effect of circMED17 overexpression on adipose tissue development in HFD-fed mice.

(a) H&E staining of iWAT from HFD-fed C57BL/6 mice after 15-day local injection of saline, empty vector (pcD2.1), or circMED17 overexpression vector (scale bar: 100 μ m).

(b) Schematic representation of circMED17 overexpression in iWAT, showing increased fat accumulation in HFD-fed mice.

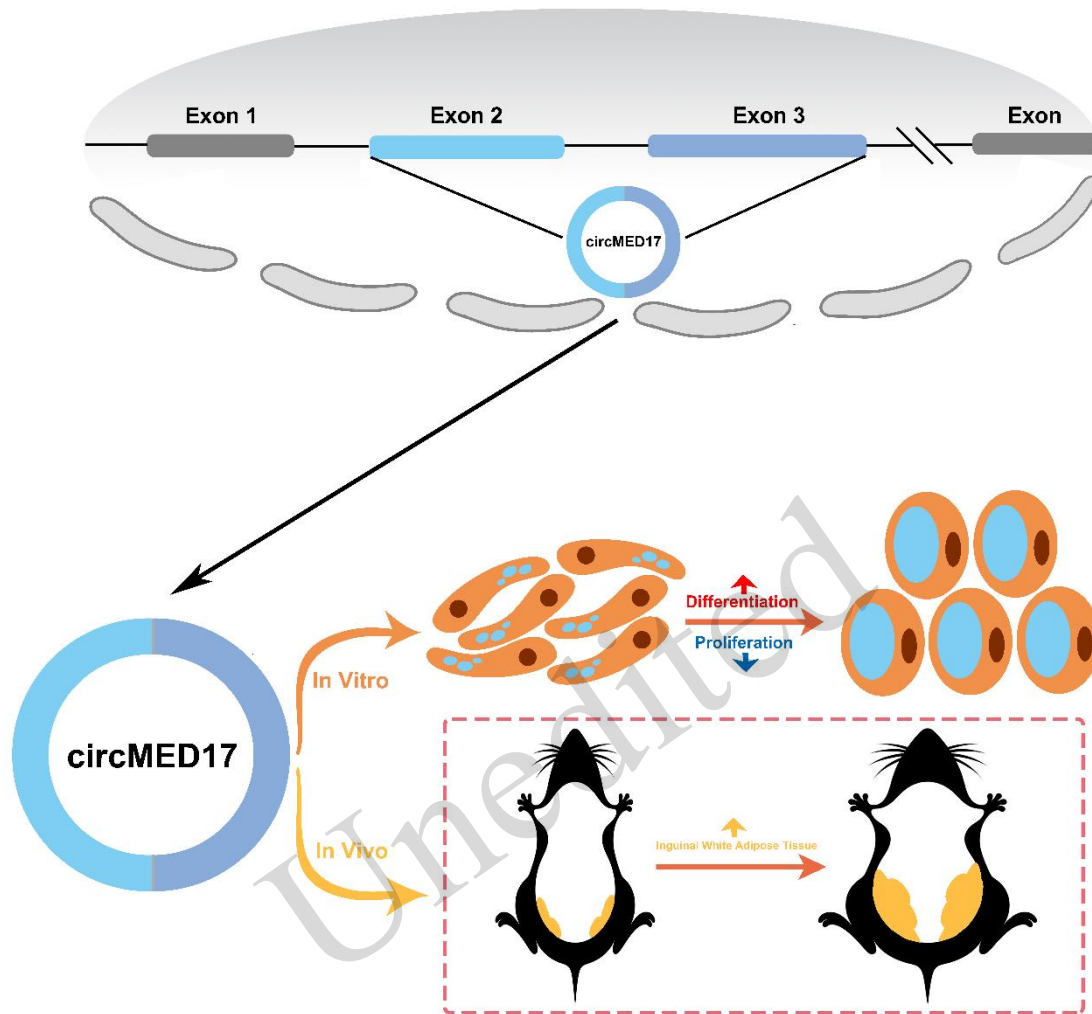


Fig.7 CircMED17 was shown to promote adipogenic differentiation in both *in vitro* and *in vivo* models.

4 Discussion

Understanding the molecular mechanisms that regulate fat deposition—an essential determinant of beef quality and economic value—is critical for elucidating adipose tissue development and identifying potential biomarkers for breeding strategies and meat quality enhancement. CircRNAs have been increasingly recognized as important regulators involved in various biological processes, including adipogenesis; therefore, investigating their role in bovine fat deposition is of great significance. To date, several circRNAs, such as circPPAR γ , circBTBD7, circCDK14, and circADAMTS16, have been reported to participate in bovine adipose development (Wu et al., 2022; Hu et al., 2023; Ma et al., 2023; Qin et al., 2025). In our previous study, circMED17 was identified as a candidate circRNA potentially involved in the regulation of adipocyte development in cattle. After confirming the circular structure of bovine circMED17, we performed quantitative expression analyses in different bovine tissues and at various stages of preadipocyte differentiation. The results showed that circMED17 was highly expressed in adipose tissue and during the later stages of preadipocyte differentiation, suggesting its potential role in adipose tissue development, particularly during the mid-to-late stages of adipocyte maturation. Based on these findings, we further conducted *in vitro* functional experiments to systematically evaluate the role of circMED17 in the proliferation and differentiation of bovine preadipocytes, as well as to explore its potential molecular regulatory mechanisms.

Preadipocyte proliferation is a critical prerequisite for adipogenesis, as a sufficient number of precursor cells is essential for subsequent differentiation and lipid accumulation. In the present study, we found that the overexpression of circMED17 significantly inhibited the proliferation of bovine preadipocytes. EdU incorporation assays revealed a marked reduction in the proportion of EdU-positive cells, accompanied by a significant downregulation of cell cycle-related genes, including *Cyclin D1* and *Cyclin E1*. These findings suggest that circMED17 may participate in the regulation of adipogenesis during the early stages of adipocyte development by restricting preadipocyte proliferation. Notably, similar functions have been reported for other circRNAs. For example, circPPARA hindered the proliferation of porcine intramuscular preadipocytes while promoting their differentiation (Li et al., 2022a); circSTX12 overexpression enhanced adipogenesis and decreased proliferative capacity (Gu et al., 2025); and circ-ATXN2 suppressed proliferation and promoted adipogenesis in rat adipose tissue (Song et al., 2021). Collectively, these findings support the concept that circRNAs, including circMED17, are important regulators in maintaining the balance between preadipocyte proliferation and differentiation during adipose tissue development. In addition to its inhibitory effect on preadipocyte proliferation, our results further demonstrate that circMED17 significantly promotes adipogenic differentiation in bovine adipocytes. Oil Red O staining revealed a substantial increase in lipid droplet accumulation in circMED17-overexpressing cells. Concurrently, the expression levels of key adipogenic marker genes, including *PPAR γ* , *C/EBP α* and *FABP4*, were significantly upregulated at both the mRNA and protein levels. These results indicate that circMED17 plays a promotive role in adipocyte differentiation. Several previous studies have confirmed the involvement of circRNAs in regulating adipocyte differentiation. For instance, the circZFYVE9/miR-378a-3p/*IMMT* axis was identified as a regulator of mitochondrial function influencing adipogenesis in 3T3-L1 preadipocytes (Qiu et al., 2024); Chi-circ_0006511 positively regulated the differentiation of goat intramuscular preadipocytes through the novel-miR-87/CD36 axis (Li et al., 2022b); and circDOCK7 promoted both proliferation and differentiation of chicken abdominal preadipocytes via the gga-miR-301b-3p/*ACSL1* axis (Tian et al., 2023). Similarly, the pro-differentiation effect of circMED17 observed in our study suggests that it may represent a broadly functional regulatory circRNA involved in adipogenesis.

CircRNAs and miRNAs are key components of non-coding RNAs (ncRNAs) that play crucial roles in regulating lipid metabolism and mitochondrial function. One of the most prominent features of circRNAs is their ability to act as “miRNA sponges,” binding to miRNAs and thereby attenuating their inhibitory effects on target genes, regulating gene expression through ceRNA mechanisms (Salmena et al., 2011). In this study, we further validated the targeting relationship between circMED17 and miR-146b using dual-luciferase reporter assays, showing that the overexpression of miR-146b directly affects circMED17 expression. RIP assays confirmed that both circMED17 and miR-146b can directly bind to the AGO2 protein, suggesting that circMED17 may modulate the physiological functions of bovine primary adipocytes by sponging miR-146b. Previous studies have demonstrated that miRNAs play important roles in adipocyte differentiation and function (Song et al., 2014; Li et al., 2017; Dong et al., 2020; Guo et al., 2021; Liu et al., 2022b). Specifically, miR-146b is a critical mediator in the regulatory network of adipose tissue, facilitating the browning of white adipocytes (Di et al., 2021) and targeting the *HOXC10* gene, which regulates cell proliferation and differentiation (Kim et al., 2019; Li et al., 2020). Moreover, miR-146b acts as a regulator of proliferation and differentiation in human visceral preadipocytes, with its expression altered in obesity; it inhibits the proliferation but promotes the differentiation of visceral preadipocytes (Chen et al., 2014). A study in 3T3-L1 cells reported that miR-146b promotes adipogenesis by targeting *SIRT1* (Ahn et al., 2013). Despite differences in cell types, the pro-adipogenic role of miR-146b appears conserved. In this study, RNA-binding protein immunoprecipitation further revealed that circMED17 directly interacts with the GATA2 protein. Previous research has reported that GATA2 inhibits the differentiation of precursor adipocytes, with its expression decreasing in early adipogenesis (Schupp et al., 2009). GATA2 likely acts as a suppressor of preadipocyte differentiation into mature adipocytes (Lin et al., 2021). As a transcription factor, GATA2 can influence the expression of adipogenic markers such as *PPAR γ* and *C/EBP α* (Sarjeant et al., 2012). GATA2 can also bind to *C/EBP α* and *C/EBP β* , disrupting their transcriptional activity (Tong et al., 2005), indicating multiple pathways by which GATA2 suppresses adipogenesis. Post-translational modifications including acetylation, sumoylation and phosphorylation further regulate GATA2 protein activity. These findings suggest that circMED17 may promote the differentiation of bovine primary adipocytes by binding to GATA2 protein and inhibiting its transcriptional and translational interference with key adipogenic genes such as *PPAR γ* .

In this study, *in vivo* experiments demonstrated that circMED17 promotes adipose tissue development, further confirming its positive regulatory role in adipogenesis. Consistent with the *in vitro* findings, adipocytes in the adipose tissue of circMED17-overexpressing mice showed significantly increased cell size, highlighting the potential of circMED17 as a key regulator of adipose development and a prospective molecular target for controlling fat deposition. To the best of our knowledge, this is the first evidence that circMED17 regulates bovine adipogenesis through a dual mechanism, acting both as a ceRNA for miR-146b and by directly binding to the GATA2 protein. Importantly, the promotive role of circMED17 in adipose tissue development was further validated *in vivo*, highlighting a previously unreported regulatory pathway in bovine adipogenesis. However, some limitations remain in the *in vitro* experiments, as the current study primarily employed overexpression models to validate circMED17 function and lacked validation through knockout or knockdown models. Additionally, although the adipocyte size was significantly increased, a comprehensive assessment involving lipid metabolism indicators, such as triglyceride content and metabolic pathway activity, was not performed. Thus, future research should further investigate the effects of circMED17 on overall energy metabolism to fully elucidate its functional mechanisms in fat metabolism and deposition.

5 Conclusion

In summary, this study comprehensively characterized the expression profile and biological functions of circMED17 in bovine adipocytes, revealing its critical regulatory roles in cell proliferation, differentiation and apoptosis. We further demonstrated that circMED17 directly targets miR-146b and binds to the GATA2 protein to exert its regulatory effects. These findings provide novel insights into the molecular mechanisms by which circMED17 regulates adipogenesis, offering a theoretical foundation for the further exploration of circRNA-mediated regulatory networks in fat development, and present a potential molecular target for improving beef quality and fine-tuning fat deposition in cattle.

Data availability statement

The data that support the findings of this study are available from the corresponding author upon reasonable request.

Acknowledgments

This work was funded by the National Natural Science Foundation of China (No.32372852), the Science Fund for Distinguished Young Scholars of Shaanxi Province (No. 2024JC-JCQN-30), the Natural Science Basic Research Program of Shaanxi Province, Key Project on Frontier Exploration (No.2025JC-QYCX-027), Natural Science Foundation of Fujian Province (No. 2024J01390).

Author contributions

Yuta YANG performed the investigation, conceptualization, methodology, software and data curation, visualization, and writing of the original draft, and participated in writing and editing the manuscript. Shaoli ZHANG participated in investigation, methodology, data curation, and contributed to writing and editing of the manuscript. Lei CHEN contributed to investigation, data analysis, and manuscript editing. Yunan HE contributed to visualization, data interpretation, and manuscript editing. Enhui JIANG participated in investigation, data interpretation, and manuscript editing. Chuanying PAN provided resources, contributed to experimental design, and manuscript editing. Yang LI provided resources and contributed to experimental design. Chuzhao LEI provided resources and contributed to experimental design. Jiyao WU contributed to funding acquisition, conceptualization, methodology, and manuscript editing. Xianyong LAN contributed to funding acquisition, project administration, supervision, and manuscript editing.

Compliance with ethics guidelines

The authors declare no conflict of interest. All animal procedures were conducted in accordance with the national guidelines for the care and use of laboratory animals and were approved by the Institutional Animal Care and Use Committee of Northwest A&F University (IACUC-NWAFU).

References

- Ahn J, Lee H, Jung CH, Jeon TI, Ha TY, 2013. MicroRNA-146b promotes adipogenesis by suppressing the SIRT1-FOXO1 cascade. *EMBO Mol Med*, 5(10):1602-1612. doi:10.1002/emmm.201302647
- Chen L, Dai YM, Ji CB, et al., 2014. MiR-146b is a regulator of human visceral preadipocyte proliferation and differentiation and its expression is altered in human obesity. *Mol Cell Endocrinol*, 393(1-2):65-74. doi:10.1016/j.mce.2014.05.022
- Di W, Zhang W, Zhu B, Li X, Tang Q, Zhou Y, 2021. Colorectal cancer prompted adipose tissue browning and cancer cachexia through transferring exosomal miR-146b-5p. *J Cell Physiol*, 236(7):5399-5410. doi:10.1002/jcp.30245
- Dong M, Ye Y, Chen Z, Xiao T, Liu W, Hu F, 2020. MicroRNA 182 is a Novel Negative Regulator of Adipogenesis by Targeting CCAAT/Enhancer-Binding Protein α . *Obesity (Silver Spring)*, 28(8):1467-1476. doi:10.1002/oby.22863
- Engin AB, 2017. MicroRNA and Adipogenesis. *Adv Exp Med Biol*, 960:489-509. doi:10.1007/978-3-319-48382-5_21
- Feng H, Yousuf S, Liu T, et al., 2022. The comprehensive detection of miRNA and circRNA in the regulation of intramuscular and subcutaneous adipose tissue of Laiwu pig. *Sci Rep*, 12(1):16542. doi:10.1038/s41598-022-21045-2
- Ferhat M, Funai K, Boudina S, 2019. Autophagy in Adipose Tissue Physiology and Pathophysiology. *Antioxid Redox Signa*, 31(6):487-501. doi:10.1089/ars.2018.7626
- Ghafouri-Fard S, Taheri M, 2021. The expression profile and role of non-coding RNAs in obesity. *Eur J Pharmacol*, 892:173809. doi:10.1016/j.ejphar.2020.173809
- Gu H, Yu W, Feng P, et al., 2025. Circular RNA circSTX12 regulates osteo-adipogenic balance and proliferation of BMSCs in senile osteoporosis. *Cell Mol Life Sci*, 82(1):149. doi:10.1007/s00018-025-05684-y
- Guo H, Khan R, Abbas Raza SH, et al., 2021. RNA-Seq Reveals Function of Bta-miR-149-5p in the Regulation of Bovine Adipocyte Differentiation. *Animals (Basel)*, 11(5):1207. doi:10.3390/ani11051207
- Hu C, Feng X, Ma Y, et al., 2023. CircADAMTS16 Inhibits Differentiation and Promotes Proliferation of Bovine Adipocytes by Targeting miR-10167-3p. *Cells*, 12(8):1175. doi:10.3390/cells12081175
- Huang CJ, Choo KB, 2023. Circular RNA- and microRNA-Mediated Post-Transcriptional Regulation of Preadipocyte Differentiation in Adipogenesis: From Expression Profiling to Signaling Pathway. *Int J Mol Sci*, 24(5):4549. doi:10.3390/ijms24054549
- Jiang EH, Zhang CY, He ZY, Zhang YL, Yang YT, Pan CY, Jiang FG, Song EL, Zhang SH, Lan XY, 2025. A novel A-to-G mutation in circBDP1 alters adipocyte proliferation and differentiation and affects bovine carcass traits. *Journal of Zhejiang University - SCIENCE B*, DOI: 10.1631/jzus.B2500084.
- Jiang R, Li H, Yang J, et al., 2020. circRNA Profiling Reveals an Abundant circFUT10 that Promotes Adipocyte Proliferation and Inhibits Adipocyte Differentiation via Sponging let-7. *Mol Ther Nucleic Acids*, 20:491-501. doi:10.1016/j.omtn.2020.03.011
- Kang Z, Zhang S, Jiang E, et al., 2020. circFLT1 and lncCCPG1 Sponges miR-93 to Regulate the Proliferation and Differentiation of Adipocytes by Promoting lncSLC30A9 Expression. *Mol Ther Nucleic Acids*, 22:484-499. doi:10.1016/j.omtn.2020.09.011
- Kim J, Bae DH, Kim JH, Song KS, Kim YS, Kim SY, 2019. HOXC10 overexpression promotes cell proliferation and migration in gastric cancer. *Oncol Rep*, 42(1):202-212. doi:10.3892/or.2019.7164
- Krüger J, Rehmsmeier M, 2006. RNAhybrid: microRNA target prediction easy, fast and flexible. *Nucleic Acids Res*, 34(Web Server issue):W451-W454. doi:10.1093/nar/gkl243
- Kuraz Abebe B, Wang J, Guo J, Wang H, Li A, Zan L, 2024. A review of the role of epigenetic studies for intramuscular fat deposition in beef cattle. *Gene*, 908:148295. doi:10.1016/j.gene.2024.148295
- Li B, He Y, Wu W, et al., 2022a. Circular RNA Profiling Identifies Novel circPPARA that Promotes Intramuscular Fat Deposition in Pigs. *J Agric Food Chem*, 70(13):4123-4137. doi:10.1021/acs.jafc.1c07358
- Li G, Ning C, Ma Y, et al., 2017. miR-26b Promotes 3T3-L1 Adipocyte Differentiation Through Targeting PTEN. *DNA Cell Biol*, 36(8):672-681. doi:10.1089/dna.2017.3712
- Li J, Tong G, Huang C, et al., 2020. HOXC10 promotes cell migration, invasion, and tumor growth in gastric carcinoma cells through upregulating proinflammatory cytokines. *J Cell Physiol*, 235(4):3579-3591. doi:10.1002/jcp.29246
- Li X, Zhang H, Wang Y, et al., 2022b. Chi-Circ_0006511 Positively Regulates the Differentiation of Goat Intramuscular Adipocytes via Novel-miR-87/CD36 Axis. *Int J Mol Sci*, 23(20):12295. doi:10.3390/ijms232012295
- Li Y, Liu Q, Pan CY, Lan XY, 2025. The free fatty acid receptor 2 (FFA2): Mechanisms of action, biased signaling, and clinical prospects. *Pharmacology & Therapeutics*, 272: 108878
- Lin T, Chen Y, Zhang Y, Li Y, Gao L, Zhang Z, 2021. Transcriptional control of chicken KLF7 promoter in preadipocytes. *Acta Biochim Biophys Sin (Shanghai)*, 53(2):149-159. doi:10.1093/abbs/gmaa149
- Liu X, Bai Y, Cui R, et al., 2022a. Sus_circPAPPA2 Regulates Fat Deposition in Castrated Pigs through the miR-2366/GK Pathway. *Biomolecules*, 12(6):753. doi:10.3390/biom12060753
- Liu X, Zhu Y, Zhan S, et al, 2022b. RNA-Seq reveals miRNA role in thermogenic regulation in brown adipose tissues of goats. *BMC Genomics*, 23(1):186. doi:10.1186/s12864-022-08401-2
- Ma Z, Chen Y, Qiu J, et al., 2023. CircBTBD7 inhibits adipogenesis via the miR-183/SMAD4 axis. *Int J Biol Macromol*, 253(Pt 2):126740. doi:10.1016/j.ijbiomac.2023.126740

Qin C, Xu F, Yue B, Zhong J, Chai Z, Wang H, 2025. SRSF3 and hnRNP A1-mediated m6A-modified circCDK14 regulates intramuscular fat deposition by acting as miR-4492-z sponge. *Cell Mol Biol Lett*, 30(1):26. doi:10.1186/s11658-025-00699-6

Qiu Y, Gan M, Wang X, et al., 2024. Whole transcriptome sequencing analysis reveals the effect of circZFYVE9/miR-378a-3p/IMMT axis on mitochondrial function in adipocytes. *Int J Biol Macromol*, 281(Pt 2):136916. doi:10.1016/j.ijbiomac.2024.136916

Ru W, Zhang S, Liu J, Liu W, Huang B, Chen H, 2023. Non-Coding RNAs and Adipogenesis. *Int J Mol Sci*, 24(12):9978. doi:10.3390/ijms24129978

Salmena L, Poliseno L, Tay Y, Kats L, Pandolfi PP, 2011. A ceRNA hypothesis: the Rosetta Stone of a hidden RNA language? *Cell*, 146(3):353-358. doi:10.1016/j.cell.2011.07.014

Sarjeant K, Stephens JM, 2012. Adipogenesis. *Cold Spring Harb Perspect Biol*, 4(9):a008417. doi:10.1101/cshperspect.a008417

Schupp M, Cristancho AG, Lefterova MI, et al., 2009. Re-expression of GATA2 cooperates with peroxisome proliferator-activated receptor-gamma depletion to revert the adipocyte phenotype. *J Biol Chem*, 284(14):9458-9464. doi:10.1074/jbc.M809498200

Song G, Xu G, Ji C, et al., 2014. The role of microRNA-26b in human adipocyte differentiation and proliferation. *Gene*, 533(2):481-487. doi:10.1016/j.gene.2013.10.011

Song XH, He N, Xing YT, et al., 2021. A Novel Age-Related Circular RNA Circ-ATXN2 Inhibits Proliferation, Promotes Cell Death and Adipogenesis in Rat Adipose Tissue-Derived Stromal Cells. *Front Genet*, 12:761926. doi:10.3389/fgene.2021.761926

Tian W, Liu Y, Zhang W, et al., 2023. CircDOCK7 facilitates the proliferation and adipogenic differentiation of chicken abdominal preadipocytes through the gga-miR-301b-3p/ACSL1 axis. *J Anim Sci Biotechnol*, 14(1):91. doi:10.1186/s40104-023-00891-8

Tong Q, Tsai J, Tan G, Dalgin G, Hotamisligil GS, 2005. Interaction between GATA and the C/EBP family of transcription factors is critical in GATA-mediated suppression of adipocyte differentiation. *Mol Cell Biol*, 25(2):706-715. doi:10.1128/MCB.25.2.706-715.2005

Toni LS, Garcia AM, Jeffrey DA, et al., 2018. Optimization of phenol-chloroform RNA extraction. *MethodsX*, 5:599-608. doi:10.1016/j.mex.2018.05.011

Wu J, Zhang S, Yue B, et al., 2022. CircRNA Profiling Reveals CircPPAR γ Modulates Adipogenic Differentiation via Sponging miR-92a-3p. *J Agric Food Chem*, 70(22):6698-6708. doi:10.1021/acs.jafc.2c01815

Yang X, Ma X, Mei C, Zan L, 2022. A genome-wide landscape of mRNAs, lncRNAs, circRNAs and miRNAs during intramuscular adipogenesis in cattle. *BMC Genomics*, 23(1):691. doi:10.1186/s12864-022-08911-z

Yousuf S, Li A, Feng H, et al., 2022. Genome-Wide Expression Profiling and Networking Reveals an Imperative Role of IMF-Associated Novel CircRNAs as ceRNA in Pigs. *Cells*, 11(17):2638. doi:10.3390/cells11172638

Zhang S, Jiang E, Kang Z, et al., 2022. CircRNA Profiling Reveals an Abundant circBDP1 that Regulates Bovine Fat Development by Sponging miR-181b/miR-204 Targeting Sirt1/TRARG1. *J Agric Food Chem*, 70(44):14312-14328. doi:10.1021/acs.jafc.2c05939

Zhao B, Zhang H, Zhao D, et al., 2023. circINSR Inhibits Adipogenic Differentiation of Adipose-Derived Stromal Vascular Fractions through the miR-152/MEOX2 Axis in Sheep. *Int J Mol Sci*, 24(4):3501. doi:10.3390/ijms24043501

Zhao X, Zhong Y, Wang X, Shen J, An W, 2022. Advances in Circular RNA and Its Applications. *Int J Med Sci*, 19(6):975-985. doi:10.7150/ijms.71840